# Association of Presynaptic Loss with Alzheimer's Disease and Cognitive Decline

Guoyu Lan, PhD,[1,2] Yue Cai, PhD,[1,2] Anqi Li, MSc,[1] Zhen Liu, PhD,[1] Shaohua Ma, PhD,[2] and Tengfei Guo, PhD,[1,3] for the Alzheimer's Disease Neuroimaging Initiative[†]

**Objective:** Increased presynaptic dysfunction measured by cerebrospinal fluid (CSF) growth-associated protein-43 (GAP43) may be observed in Alzheimer's disease (AD), but how CSF GAP43 increases relate to AD-core pathologies, neurodegeneration, and cognitive decline in AD requires further investigation.
**Methods:** We analyzed 731 older adults with baseline β-amyloid (Aβ) positron emission tomography (PET), CSF GAP43, CSF phosphorylated tau181 (p-$Tau_{181}$), and $^{18}$F-fluorodeoxyglucose PET, and longitudinal residual hippocampal volume and cognitive assessments. Among them, 377 individuals had longitudinal $^{18}$F-fluorodeoxyglucose PET, and 326 individuals had simultaneous longitudinal CSF GAP43, Aβ PET, and CSF p-$Tau_{181}$ data. We compared baseline and slopes of CSF GAP43 among different stages of AD, as well as their associations with Aβ PET, CSF p-$Tau_{181}$, residual hippocampal volume, $^{18}$F-fluorodeoxyglucose PET, and cognition cross-sectionally and longitudinally.
**Results:** Regardless of Aβ positivity and clinical diagnosis, CSF p-$Tau_{181}$-positive individuals showed higher CSF GAP43 concentrations ($p < 0.001$) and faster rates of CSF GAP43 increases ($p < 0.001$) compared with the CSF p-$Tau_{181}$-negative individuals. Moreover, higher CSF GAP43 concentrations and faster rates of CSF GAP43 increases were strongly related to CSF p-$Tau_{181}$ independent of Aβ PET. They were related to more rapid hippocampal atrophy, hypometabolism, and cognitive decline ($p < 0.001$), and predicted the progression from MCI to dementia (area under the curve for baseline 0.704; area under the curve for slope 0.717) over a median 4 years of follow up.
**Interpretation:** Tau aggregations rather than Aβ plaques primarily drive presynaptic dysfunction measured by CSF GAP43, which may lead to sequential neurodegeneration and cognitive impairment in AD or neurodegenerative diseases.

ANN NEUROL 2022;00:1–15

## Introduction

The aggregation of extracellular β-amyloid (Aβ) plaques and intraneuronal neurofibrillary tau tangles are the two key hallmarks of Alzheimer's disease (AD),[1] which can be detected directly by positron emission tomography (PET) imaging[2, 3] or indirectly by CSF $A\beta_{42}/A\beta_{40}$ ratio and phosphorylated tau (p-Tau) biomarkers.[4, 5] According to the biological definition of AD[6] and recent reports,[7–10] Aβ (A) pathology presents initially in disease onset, followed by tau (T) aggregation, which subsequently results in neurodegeneration (N) and cognitive decline. However, several recent studies[11–13] also identified different A/T/N profiles with overlapping features of neurodegeneration and cognitive decline, indicating we may need extra techniques beyond A/T/N biomarkers to understand the progression of the disease fully.[14]

Synaptic impairment appears closely linked to neurodegeneration and cognitive decline in AD.[15–17] One

View this article online at wileyonlinelibrary.com. DOI: 10.1002/ana.26492

Received Jun 6, 2022, and in revised form Aug 22, 2022. Accepted for publication Aug 24, 2022.

Address correspondence to Dr Tengfei Guo, Institute of Biomedical Engineering, Shenzhen Bay Laboratory, No.5 Kelian Road, Shenzhen, 518132, China. E-mail: tengfei.guo@szbl.ac.cn

[†]Data used in preparation of this article were obtained from the Alzheimer's Disease Neuroimaging Initiative (ADNI) database (adni.loni.usc.edu). As such, the investigators within the ADNI contributed to the design and implementation of ADNI and/or provided data, but did not participate in analysis or writing of this report. A complete listing of ADNI investigators can be found at: http://adni.loni.usc.edu/wp-content/uploads/how_to_apply/ADNI_Acknowledgement_List.pdf.

From the [1]Institute of Biomedical Engineering, Shenzhen Bay Laboratory, Shenzhen, China; [2]Tsinghua Shenzhen International Graduate School (SIGS), Tsinghua University, Shenzhen, China; and [3]Institute of Biomedical Engineering, Peking University Shenzhen Graduate School, Shenzhen, China

 

meta-analysis study[16] suggested presynaptic markers may be affected more than postsynaptic markers in AD. Growth-associated protein-43 (GAP43) is a presynaptic membrane protein primarily expressed in the hippocampus and associated cortex, and participates in the regulation of synaptogenesis, synaptic plasticity, and axon outgrowth in the adult brain.[18, 19] Post-mortem studies showed an apparent decrease in GAP43 expression in the frontal cortex and some hippocampal areas of AD brains.[20, 21] At the same time, emerging evidence proved that CSF GAP43 concentrations increased in AD, but not in other neurodegenerative disorders.[22, 23] However, two recent cross-sectional studies[24, 25] reported conflicting findings about the associations among Aβ, tau, and CSF GAP43 dysfunction in AD. Specifically, the former[24] did not observe a significant difference between A + /T– and A−/T– in individuals with mild cognitive impairment (MCI), whereas the latter[25] found elevated CSF GAP43 concentrations in A + /T– group compared with the A−/T– group among cognitively unimpaired (CU) individuals. Consequently, the mechanism of GAP43 dysfunction during AD pathogenesis remains elusive.

In the present study, we compared CSF GAP43 among different clinical (CU, MCI, and dementia) and biological (A/T) stages of AD using both cross-sectional and longitudinal data from the Alzheimer's Disease Neuroimaging Initiative (ADNI) cohort. We also investigated the cross-sectional and longitudinal associations of CSF GAP43 with Aβ, tau, neurodegeneration, and cognitive decline in different Aβ positivity and clinical stages. We aimed to investigate the alterations of CSF GAP43 among different stages of AD, the associations of Aβ and tau pathologies with CSF GAP43, and the prediction of CSF GAP43 on longitudinal neurodegeneration and cognitive decline. The ultimate goal is to help understand the mechanisms underlying presynaptic loss, and how synaptic dysfunction results in neurodegeneration and cognitive decline in AD.

## Methods

### Participants

Data used in the preparation of this article were obtained from the ADNI database (adni.loni.usc.edu). The ADNI was launched in 2003 as a public–private partnership, led by Principal Investigator Michael W. Weiner, MD. The primary goal of ADNI is to test whether serial magnetic resonance imaging (MRI), PET, other biological markers, and clinical and neuropsychological assessment can be combined to measure the progression of MCI and early AD. The ADNI study was approved by the institutional review boards of all participating centers, and written informed consent was obtained from all participants or their authorized representatives.

We identified 731 participants (232 CU, 395 MCI, and 104 dementia) with baseline $^{18}$F-florbetapir (FBP) Aβ PET and concurrent (within 1 year) CSF GAP43, CSF p-Tau$_{181}$, and $^{18}$F-fluorodeoxyglucose (FDG) PET, as well as longitudinal structure MRI (median 2.0 years, [interquartile range (IQR) 3.1 years of follow-up) and cognitive assessments (median 4.0 years [IQR 5.0 years] of follow up). Among them, 377 individuals had longitudinal FDG PET (median 2.0 years [IQR 2.4 years) of follow up), and 326 individuals had simultaneous longitudinal CSF GAP43, Aβ PET, and CSF p-Tau$_{181}$ data. In addition, 233 individuals had concurrent longitudinal CSF GAP43, Aβ PET, CSF p-Tau$_{181}$, and FDG PET data.

### CSF Biomarkers

CSF GAP43 was detected by an in-house enzyme-linked immunosorbent assay method at the Clinical Neurochemistry Laboratory of the Sahlgrenska University Hospital (Mölndal, Sweden), as described previously.[22] CSF p-Tau$_{181}$ was analyzed by the ADNI biomarker core group using the fully automated Roche Elecsys.[26] The threshold of CSF p-Tau$_{181}$ positivity (T +) was defined as ≥23pg/ml according to the receiver operating characteristic analysis using the Youden index, classifying 326 Aβ– ADNI CU participants and 467 Aβ+ ADNI MCI and dementia patients as the end-point (area under the curve [AUC] 0.86, 95% confidence interval [95% CI] 0.84–0.89). Linear mixed effect (LME) models were used to calculate slopes of CSF GAP43 (ΔCSF GAP43) and CSF p-Tau$_{181}$ (ΔCSF p-Tau$_{181}$) for all the participants with longitudinal CSF data, adjusting for age and sex, and including a random slope and intercept.

### PET and MRI Imaging Processing

FBP PET and FDG PET data were acquired from 50 to 70 min (FBP, 4 × 5-min frames) and 30–60 min (FDG, 6 × 5-min frames) post-injection. PET images were motion corrected, time-averaged, and summed into one static frame, and more details are given elsewhere (http://adni-info.org).

FBP image was coregistered to their corresponding structural MRI scan that was closest in time to the PET scan. Cortical florbetapir uptake in 68 FreeSurfer-defined regions of interest defined by the Desikan–Killiany atlas[27] were extracted using FreeSurfer (v7.1.1). A cortical summary composite standardized uptake value ratio (SUVR) was calculated by referring FBP uptake in AD summarized cortical regions (including frontal, cingulate, parietal, and temporal regions) to the mean uptake of the whole cerebellum.[28] The Aβ+ of FBP PET was defined as composite

SUVR ≥1.11.[28] SUVRs that referred to one composite reference region (made up of the brainstem, whole cerebellum, and eroded white matter)[28] were used to calculate slopes of FBP SUVR (ΔAβ PET) for all the participants with longitudinal FBP PET data using LME models, adjusting for age and sex, and including a random slope and intercept.

FDG images were spatially normalized in SPM12 to the MNI PET template. FDG SUVR in a pre-defined MetaROIs (made up of left angular gyrus, right angular gyrus, bilateral posterior cingulate, left inferior temporal gyrus, and right inferior temporal gyrus) were calculated by normalizing averaging FDG counts in MetaROIs to that found in the upper 50% of voxels in a pons/vermis reference region.[29] Slopes of FDG SUVR (ΔFDG PET) were calculated for all the participants with longitudinal FDG PET data using LME models, adjusting for age and sex, and including a random slope and intercept.

Hippocampal volume (HCV; $cm^3$) was computed across hemispheres from the structural MRI scan via FreeSurfer, and adjusted by the estimated intracranial volume using the approach reported by Jack et al.[30] The residual HCV (rHCV) was calculated as the difference between the raw and expected HCV, as we described previously.[8] Slopes of rHCV (ΔrHCV) were calculated for all the participants with longitudinal MRI data using LME models, adjusting for age and sex, and including a random slope and intercept.

### Biological Stages Defined by A/T Biomarkers

Participants were classified into four different A/T profiles according to the abnormal status of Aβ PET (A±) and CSF p-$Tau_{181}$ (T±) defined by the cut-off values as described above. For sensitivity analysis, we also used an alternative cut-off for CSF p-$Tau_{181}$ ≥19.2pg/ml[31] reported by a different cohort to define T±.

### Cognitive Assessments

Previously validated preclinical Alzheimer cognitive composite (PACC)[32] scores were used to represent global cognition. Briefly, PACC scores were computed by combining z-scores of several cognitive tests, including the delayed recall portion of the Alzheimer's Disease Assessment Scale, the delayed recall score on the logical memory IIa subtest from the Wechsler Memory Scale, the digit symbol substitution test score from the Wechsler Adult Intelligence Scale-Revised, and the Mini-Mental State Examination total score as described previously.[8] Slopes of PACC scores (ΔPACC scores) were calculated for all the participants with longitudinal PACC data using LME models, adjusting for age, sex and education, and including a random slope and intercept.

### Statistical Analysis

All statistical analyses were performed using R version 4.1.1 (The R Foundation for Statistical Computing, Vienna, Austria). Due to the limited sample size of dementia patients in some subsets, we combined MCI and dementia into the cognitively impaired (CI) group in our primary analysis. Data are presented as the median (IQR) or number (%), unless otherwise noted. A two-tailed significance level of $p < 0.05$ was applied if not otherwise stated. The characteristics at baseline of Aβ– CU, Aβ– CI, Aβ+ CU, and Aβ+ CI groups were compared by using a two-tailed Mann–Whitney *U* test or Fisher's exact test. A false discovery rate (FDR) of 0.05 was applied using the Benjamini–Hochberg approach for multiple comparisons correction.

We used generalized linear models to determine the associations of baseline CSF GAP43 and ΔCSF GAP43 with age, sex, and *APOE*-ε4 status. Generalized linear models were also used to compare baseline CSF GAP43 and ΔCSF GAP43 among clinical groups, Aβ positivity/clinical groups, and A/T groups, controlling for age, sex, and *APOE*-ε4 status Benjamini–Hochberg's approach was used for multiple comparisons correction (FDR <0.05).

To further explore the independent influence of Aβ and tau pathologies on CSF GAP43, we subsequently investigated the prediction of baseline CSF GAP43 and ΔCSF GAP43 by including Aβ PET and CSF p-$Tau_{181}$ as the predictors in one multivariate model in Aβ– CU, Aβ– CI, Aβ+ CU, and Aβ+ CI groups separately, controlling for the same covariates above.

To determine the predictive effect of CSF GAP43 on the disease progression, we used generalized linear models to investigate the associations of baseline CSF GAP43 and ΔCSF GAP43 with ΔrHCV, ΔFDG PET, and ΔPACC scores, controlling for the same covariates above. Additionally, we conducted a receiver operating characteristic curve analysis to investigate whether CSF GAP43 can predict the conversion from MCI to dementia at follow up. Finally, mediation analysis (R; Lavaan package)[33] was conducted to explore the sequential associations among longitudinal changes of CSF p-$Tau_{181}$, CSF GAP43, rHCV, and PACC scores.

## Results

### Demographics

The characteristics at baseline of participants are summarized in Table . Among 731 participants, 347 (48%) were women, 398 (54%) were *APOE*-ε4 carriers, 393 (54%) were Aβ positive, and 499 (68%) were CI and the median age was 72.6 years (IQR 10.3 years). Longitudinal data of CSF GAP43, Aβ PET, CSF p-$Tau_{181}$, rHCV, FDG PET,

**TABLE. Demographics of Participants**

| Characteristic at baseline | Aβ– CU | Aβ– CI | Aβ+ CU | Aβ+ CI |
|---|---|---|---|---|
| No. patients (%) | 154 (21) | 184 (25) | 78 (11) | 315 (43) |
| Age (years) | 71.5 (8.6) | 69.8 (12.2) | 75.2 (9.0)[a,b] | 73.7 (9.8)[b,d,f] |
| Female, *n* (%) | 75 (49) | 82 (45) | 53 (68)[d,e] | 137 (43)[c] |
| Education, years | 17 (2.8) | 16 (4.0)[d] | 16 (4.0) [d] | 16 (4.0)[a] |
| CSF p-Tau$_{181}$ positive, *n* (%) | 37 (24) | 40 (22) | 41 (53)[a,b] | 242 (77)[a,b,c] |
| APOE-ε4 carriers, *n* (%) | 33 (21) | 46 (25) | 33 (42)[a,e] | 221 (70)[a,b,c] |
| Aβ PET SUVR | 1.02 (0.08) | 1.01 (0.07) | 1.29 (0.21)[a,b] | 1.40 (0.26)[a,b,c] |
| CSF p-Tau$_{181}$ (pg/ml) | 17.7 (7.8) | 17.7 (9.0) | 24.1 (13.3)[a,b] | 31.3 (18.4)[a,b,c] |
| CSF GAP43 (pg/ml) | 4,096 (2809) | 3,747 (2386) | 4756 (3909)[b] | 5243 (3998)[a,b] |
| rHCV (cm$^3$) | −0.02 (0.47) | −0.11 (0.68)[d] | −0.11 (0.51) [d] | −0.44 (0.62)[a,b,c] |
| FDG PET SUVR (MetaROIs) | 1.30 (0.13) | 1.27 (0.17)[d] | 1.28 (0.19)[d] | 1.16 (0.21) [a, b, c] |
| PACC scores | 0.76 (3.44) | −3.42 (4.72)[a] | −0.31 (3.86)[b] | −9.28 (9.71)[a,b,c] |
| **326 participants with concurrent longitudinal Aβ PET, CSF p-Tau$_{181}$, CSF GAP43, MRI, and PACC data** | | | | |
| No. patients (%) | 83 (25) | 81 (25) | 44 (14) | 118 (36) |
| Visits of CSF GAP43, median (IQR, range) | 2.0 (1.0, 2–3) | 2.0 (1.0, 2–4) | 2.0 (1.0, 2–3) | 2.0 (1.0, 2–3) |
| Duration of CSF GAP43, years, median (IQR, range) | 2.0 (2.0, 1.3–4.3) | 3.1 (2.0, 1.7–6.0) | 2.2 (2.0, 1.9–5.0) | 2.0 (2.0, 1.7–5.0) |
| Visits of Aβ PET, median (IQR, range) | 3.0 (1.5, 2–6) | 4.0 (2.0, 2–6) | 3.0 (1.3, 2–5) | 3.0 (1.0, 2–6) |
| Duration of Aβ PET, years, median (IQR, range) | 5.9 (4.4, 1.9–10.0) | 6.0 (4.0, 1.9–10.2) | 5.0 (3.0, 1.9–9.0) | 4.0 (3.1, 1.9–9.2) |
| Visits of CSF p-Tau$_{181}$, median (IQR, range) | 2.0 (1.5, 2–5) | 3.0 (2.0, 2–5) | 3.0 (2.0, 2–5) | 2.0 (1.0, 2–4) |
| Duration of CSF p-Tau$_{181}$, years, median (IQR, range) | 2.4 (3.3, 1.5–8.5) | 4.0 (4.3, 1.7–9.1) | 4.0 (3.7, 1.9–8.6) | 2.1 (2.0, 1.7–8.4) |
| Visits of MRI, median (IQR, range) | 4.0 (2.0, 2–9) | 5.0 (3.0, 2–12) | 4.0 (2.0, 2–8) | 5.0 (2.0, 2–11) |
| Duration of MRI, years, median (IQR, range) | 2.1 (4.6, 0.4–10.2) | 4.0 (6.0, 0.8–11.2) | 2.3 (4.7, 0.2–8.1) | 2.1 (3.0, 0.5–9.9) |
| Visits of PACC, median (IQR, range) | 6.0 (2.0, 3–9) | 8.0 (4.0, 3–13) | 6.0 (2.0, 3–10) | 6.0 (2.0, 4–12) |
| Duration of PACC, years, median (IQR, range) | 6.5 (4.2, 1.9–10.5) | 7.0 (4.5, 2.0–11.2) | 5.8 (4.0, 2.0–9.9) | 4.1 (2.5, 1.9–11.0) |
| **233 participants with longitudinal FDG PET** | | | | |
| No. patients (%) | 49 (21) | 67 (29) | 29 (12) | 88 (38) |
| Visits of FDG PET, median (IQR, range) | 2.0 (0, 2–3) | 2.0 (1, 2–3) | 2.0 (0, 2–3) | 2.0 (0, 2–3) |
| Duration of FDG PET, years, median (IQR, range) | 2.0 (0.1, 1.5–6.8) | 3.2 (4.2, 1.9–8.2) | 2.0 (0.1, 1.9–7.1) | 2.0 (2.9, 1.9–7.5) |

Abbreviations: *APOE*, apolipoprotein E; CI, cognitively impaired; CU, cognitively unimpaired; GAP43, growth-associated protein-43; IQR, interquartile range; MetaROIs, left angular gyrus, right angular gyrus, bilateral posterior cingulate, left inferior temporal gyrus, right inferior temporal gyrus; PACC, Preclinical Alzheimer Cognitive Composite; p-Tau$_{181}$, phosphorylated tau181; rHCV, residual hippocampal volume; SUVR, standard uptake value ratio. Data are presented as median (IQR) or number (%). Multiple comparisons correction was used (false discovery rate <0.05).

[a] $p$ <0.001 versus Aβ– CU.
[b] $p$ <0.001 versus Aβ– CI.
[c] $p$ <0.001 versus Aβ+ CU.
[d] $p$ <0.05 versus Aβ– CU.
[e] $p$ <0.05 versus Aβ– CI.
[f] $p$ <0.05 versus Aβ+ CU.

and PACC scores are also illustrated in Table . In the whole cohort, older ages were associated with higher baseline CSF GAP43 (standardized β [$\beta_{std}$] = 0.12 [95% CI 0.05–0.19], $p$ = 0.001), but not with ΔCSF GAP43. *APOE*-ε4 carriers had higher baseline CSF GAP43 (estimate = 1,089 [95% CI 0.24–0.53], $p < 0.001$) and faster ΔCSF GAP43 increases (estimate = 29 [95% CI 0.27–0.71], $p < 0.001$) than *APOE*-ε4 non-carriers.

### Comparison of CSF GAP43 among Different Clinical and Biological Stages of AD

At baseline, the dementia group had higher CSF GAP43 concentrations than the MCI group (estimate = 847 [95% CI 0.08–0.51], $p$ = 0.007) and CU group (estimate = 965 [95% CI 0.10–0.57], $p$ = 0.007; Fig 1A). After stratified by Aβ positivity, higher CSF GAP43 concentrations were found in Aβ– dementia (estimate = 2,452 [95% CI 0.30–1.43], $p$ = 0.005), Aβ+ MCI (estimate = 1,144 [95% CI 0.19–0.61], $p < 0.001$), and Aβ+ dementia (estimate = 1,273 [95% CI 0.18–0.71], $p$ = 0.002), but not in Aβ– MCI and Aβ+ CU groups compared with the Aβ– CU individuals (Fig 1B). Longitudinally, only Aβ+ MCI individuals showed faster ΔCSF GAP43 increases (estimate = 31 [95% CI 0.22–0.82], $p$ = 0.004) than the Aβ– CU group (Fig 2B). Notably, we also observed marginally higher CSF GAP43 concentrations (estimate = 694 [95% CI −0.02 to 0.51], $p$ = 0.079) in Aβ+ CU individuals than Aβ– CU individuals.

To further explore the associations of CSF GAP43 with Aβ and tau pathologies, we compared cross-sectional and longitudinal CSF GAP43 among different A/T profiles. Notably, both A−/T + and A + /T + had significantly higher CSF GAP43 concentrations than the A−/T– and A + /T– groups regardless of clinical status (Fig 1C). Similar to baseline, significantly faster ΔCSF GAP43 increases were also found in A−/T + and A + /T + groups compared with the A−/T– and A + /T– groups (Fig 2C).

Additionally, the results were duplicated using the alternative cut-off for CSF p-$Tau_{181}$ to define tau-positivity (T±).

### Association of CSF GAP43 with Aβ PET and CSF p-$Tau_{181}$

Regardless of Aβ and clinical status, higher CSF p-$Tau_{181}$ concentrations were related to greater baseline CSF GAP43 (Aβ– CU: $\beta_{std}$ = 0.72 [95% CI 0.61–0.84], $p < 0.001$; Aβ– CI: $\beta_{std}$ = 0.78 [95% CI 0.68–0.87], $p < 0.001$; Aβ+ CU: $\beta_{std}$ = 0.66 [95% CI 0.48–0.84], $p < 0.001$; Aβ+ CI: $\beta_{std}$ = 0.76 [95% CI 0.68–0.83], $p < 0.001$) and faster ΔCSF GAP43 increases (Aβ– CU: $\beta_{std}$ = 0.73 [95% CI 0.57–0.88], $p < 0.001$; Aβ– CI: $\beta_{std}$ = 0.77 [95% CI 0.61–0.93], $p < 0.001$; Aβ+ CU: $\beta_{std}$ = 0.75 [95% CI 0.52–0.97], $p < 0.001$; Aβ+ CI: $\beta_{std}$ = 0.73 [95% CI 0.60–0.86], $p < 0.001$; Fig 3A–D). When additionally controlling for baseline CSF GAP43 concentrations, higher CSF p-$Tau_{181}$ concentrations were still related to faster ΔCSF GAP43 increases in Aβ– CU ($\beta_{std}$ = 0.16 [95% CI 0.04–0.28], $p$ = 0.009), Aβ– CI ($\beta_{std}$ = 0.16 [95% CI 0.03–0.29], $p$ = 0.019) and Aβ+ CU ($\beta_{std}$ = 0.22 [95% CI 0.08–0.36], $p$ = 0.002), but not in Aβ+ CI.

Moreover, ΔCSF p-$Tau_{181}$, but not ΔAβ PET were positively associated with faster ΔCSF GAP43 increases in all subgroups (Aβ– CU: $\beta_{std}$ = 0.54 [95% CI 0.34–0.74], $p < 0.001$; Aβ– CI: $\beta_{std}$ = 0.47 [95% CI 0.24–0.69], $p < 0.001$; Aβ+ CU: $\beta_{std}$ = 0.57 [95% CI 0.30–0.84], $p < 0.001$; Aβ+ CI: $\beta_{std}$ = 0.50 [95% CI 0.34–0.66], $p < 0.001$; Fig 3E,F). Only in Aβ+ CI did the positive link ($\beta_{std}$ = 0.16 [95% CI 0.10–0.22], $p < 0.001$) between ΔCSF p-$Tau_{181}$ and ΔCSF GAP43 persist after adjusting for baseline levels of Aβ PET, CSF p-$Tau_{181}$, and CSF GAP43.

### Association of CSF GAP43 with Longitudinal Neurodegeneration and Cognitive Decline

In the whole cohort, higher baseline CSF GAP43 concentrations were associated with faster ΔrHCV decreases (Fig 4A; $\beta_{std}$ = −0.15 [95% CI −0.22 to −0.08], $p < 0.001$) and ΔPACC scores decreases (Fig 4E; $\beta_{std}$ = −0.19 [95% CI −0.26 to −0.12], $p < 0.001$). Likewise, faster ΔCSF GAP43 increases were also related to faster ΔrHCV decreases (Fig 4B; $\beta_{std}$ = −0.23 [95% CI −0.33 to −0.12], $p < 0.001$) and ΔPACC scores decreases (Fig 4F; $\beta_{std}$ = −0.19 [95% CI −0.29 to −0.08], $p < 0.001$). After stratified by Aβ and cognition status, higher baseline CSF GAP43 concentrations ($\beta_{std}$ = −0.15 [95% CI −0.25 to −0.04], $p$ = 0.008) and faster ΔCSF GAP43 increases ($\beta_{std}$ = −0.25 [95% CI −0.42 to −0.07], $p$ = 0.006) were related to faster ΔrHCV decreases only in Aβ+ CI. In addition, baseline CSF GAP43 concentrations, but not ΔCSF GAP43, were negatively associated with faster ΔPACC scores decreases in Aβ– CI ($\beta_{std}$ = −0.19 [95% CI −0.34 to −0.05], $p$ = 0.008) and Aβ+ CI ($\beta_{std}$ = −0.13 [95% CI −0.24 to −0.02], $p$ = 0.019). In the subgroups of individuals with longitudinal FDG PET scan, both higher baseline CSF GAP43 (Fig 4C; $\beta_{std}$ = −0.19 [95% CI −0.29 to −0.09], $p < 0.001$, n = 377) and faster ΔCSF GAP43 increases (Fig 4D; $\beta_{std}$ = −0.19 [95% CI −0.32 to −0.06], $p$ = 0.003, n = 233) were associated with faster ΔFDG PET decreases. When stratified by Aβ and cognition status, the link between baseline or longitudinal CSF

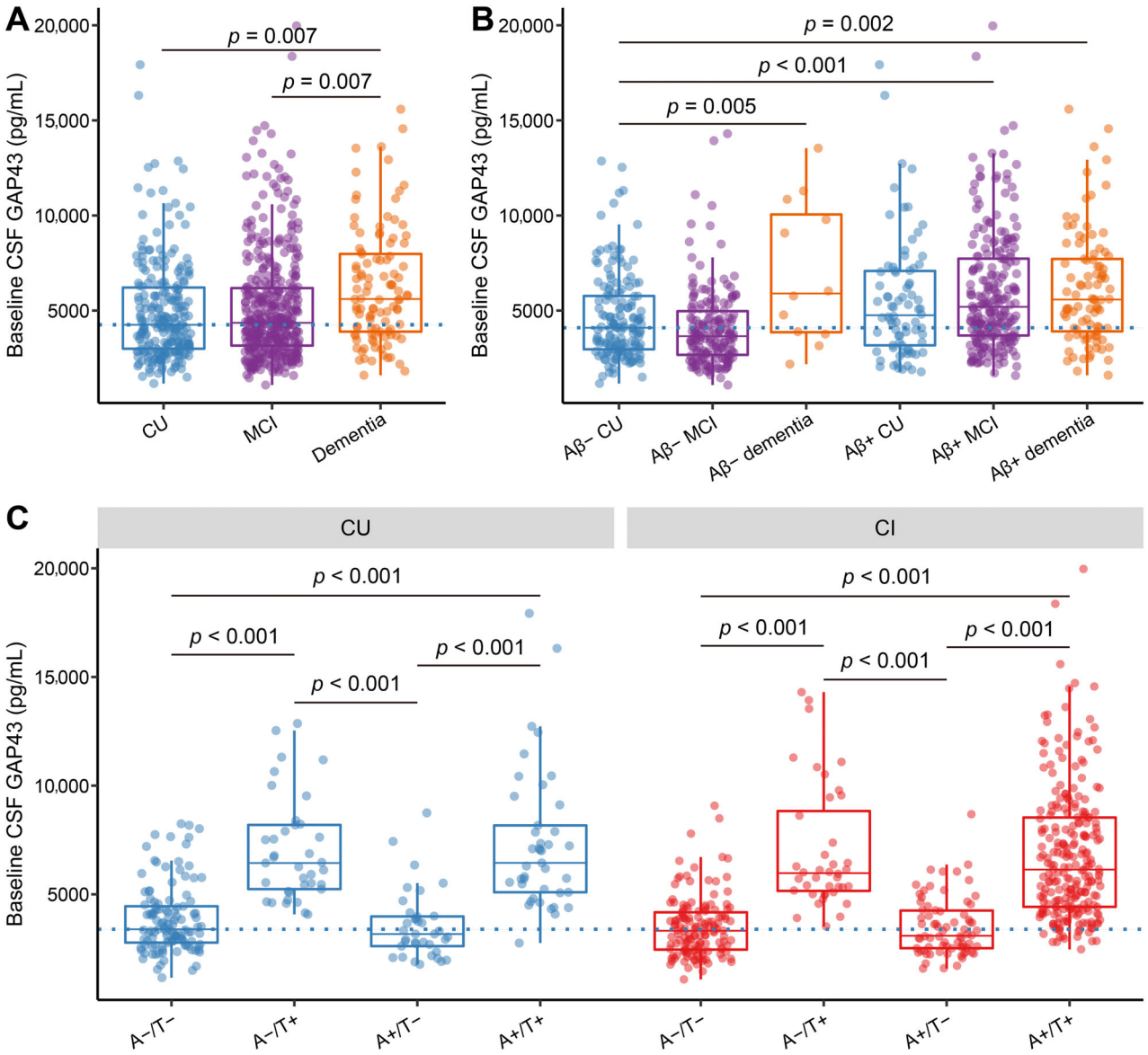


**FIGURE 1: Comparison of baseline CSF GAP43 among different clinically- and biologically-defined stages of AD. Comparison of baseline CSF GAP43 among (A) different clinical diagnosis groups, (B) different Aβ positivity and clinical diagnosis groups, and (C) different A/T groups. The boxplots show the median (horizontal bar), interquartile range (IQR; hinges), and 1.5 × IQR (whiskers). Each point represents an individual, and dashed lines represent the median values of the CU, Aβ− CU, or A−/T− CU group. The *p* values of the comparisons are shown at the top, adjusting for age, sex, and *APOE*-ε4 status. Multiple comparisons correction was performed using the Benjamini–Hochberg method (FDR <0.05). The estimates of baseline CSF GAP43 in the CU group: A−/T + versus A−/T− (estimate = 3,161 [95% CI 0.90–1.49], *p* < 0.001), A−/T + versus A + /T− (estimate = 3,446 [95% CI 0.94–1.67], *p* < 0.001), A + /T + versus A−/T− (estimate = 3,537 [95% CI 1.03–1.65], *p* < 0.001), A + /T + versus A + /T− (estimate = 3,822 [95% CI 1.09–1.80], *p* < 0.001); The estimates of baseline CSF GAP43 in CI group: A−/T + versus A−/T− (estimate = 3,557 [95% CI 0.92–1.50], *p* < 0.001), A−/T + versus A + /T− (estimate = 3,601 [95% CI 0.91–1.55], *p* < 0.001), A + /T + versus A−/T− (estimate = 3,221 [95% CI 0.90–1.29], *p* < 0.001), A + /T + versus A + /T− (estimate = 3,265 [95% CI 0.89–1.33], *p* < 0.001). A = Aβ; Aβ = β-amyloid; AD = Alzheimer's disease; CSF = cerebrospinal fluid; CU = cognitively unimpaired; FDR = false discovery rate; GAP43 = growth-associated protein-43; MCI = mild cognitive impairment; N = neurodegeneration; T = tau.**

GAP43 and longitudinal FDG PET was eliminated, which may result from the small number of individuals in each category.

Among 181 MCI individuals with a median (IQR) of 4.0 (2.0) years of follow-up clinical assessments, we found 136 remained stable (MCI-MCI), whereas 45 progressed to dementia (MCI-Dementia). The MCI-Dementia group had higher baseline CSF GAP43 (Fig 5A; estimate = 1,617 [95% CI 0.20–0.86], $p = 0.002$) and faster ΔCSF GAP43 increases (Fig 5B; estimate = 34 [95% CI 0.24–0.90], $p < 0.001$) than the MCI-MCI group. Additionally, the receiver operating

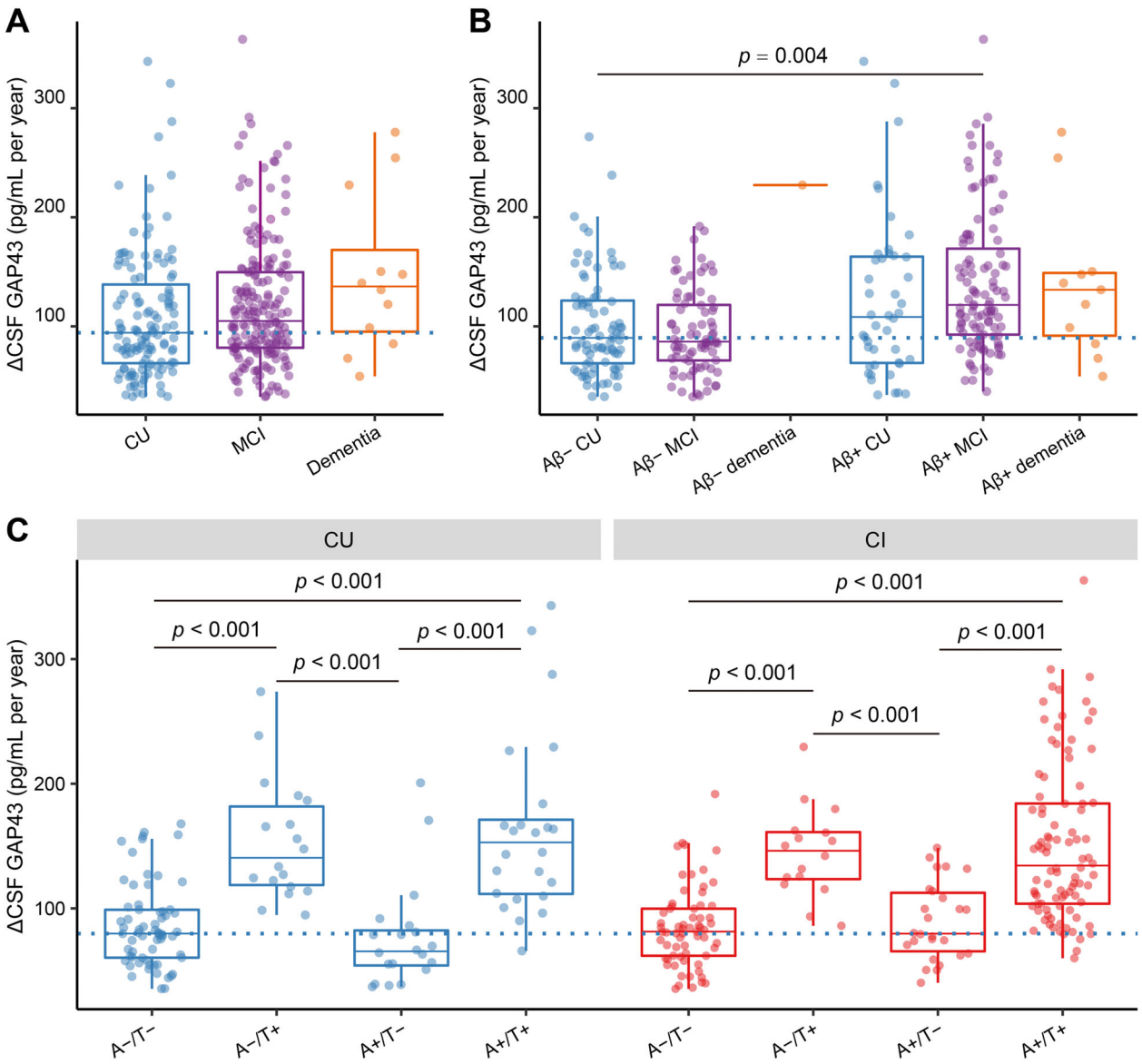


**FIGURE 2: Comparison of longitudinal CSF GAP43 changes among different clinically- and biologically-defined stages of AD. Comparison of CSF GAP43 slopes (ΔCSF GAP43) among (A) different diagnosis groups, (B) different Aβ positivity and diagnosis groups, and (C) different A/T groups. The boxplots show the median (horizontal bar), interquartile range (IQR; hinges), and 1.5 × IQR (whiskers). Each point represents an individual, and dashed lines represent the median values of the CU, Aβ− CU, or A−/T− CU group. The *p* values of the comparisons are shown at the top, adjusting for age, sex, and *APOE*-ε4 status. Multiple comparisons correction was performed using the Benjamini–Hochberg method (FDR <0.05). The estimates of CSF GAP43 slopes in the CU group: A−/T + versus A−/T− (estimate = 69 [95% CI 0.75–1.60], *p* < 0.001), A−/T + versus A + /T− (estimate = 72 [95% CI 0.71–1.76], *p* < 0.001), A + /T + versus A−/T− (estimate = 85 [95% CI 1.03–1.87], *p* < 0.001), A + /T + versus A + /T− (estimate = 88 [95% CI 1.03–1.99], *p* < 0.001); The estimates of CSF GAP43 slopes in CI group: A−/T + versus A−/T− (estimate = 61 [95% CI 0.57–1.50], *p* < 0.001), A−/T + versus A + /T− (estimate = 62 [95% CI 0.51–1.58], *p* < 0.001), A + /T + versus A−/T- (estimate = 64 [95% CI 0.77–1.39], *p* < 0.001), A + /T + versus A + /T− (estimate = 64 [95% CI 0.72–1.45], *p* < 0.001). A = Aβ; Aβ = β-amyloid; AD = Alzheimer's disease; CSF = cerebrospinal fluid; CU = cognitively unimpaired; FDR = false discovery rate; GAP43 = growth-associated protein-43; MCI = mild cognitive impairment; N = neurodegeneration; T = tau.**

characteristic analyses showed that baseline CSF GAP43 (Fig 5C; AUC = 0.704 [95% CI 0.61–0.79], sensitivity = 76.5%, specificity = 62.2%) and ΔCSF GAP43 (Fig 5D; AUC = 0.717 [95% CI 0.63–0.80], sensitivity = 68.1%, specificity = 71.1%) could significantly identify MCI progressors.

### *Mediation Analysis among Longitudinal CSF p-Tau$_{181}$, CSF GAP43, Hippocampal Volume, and Cognition*

Among 326 individuals with longitudinal data, faster ΔCSF p-Tau$_{181}$ increases were negatively related to ΔrHCV ($\beta_{std}$ = −0.18 [95% CI −0.28 to −0.07], *p* = 0.001) and

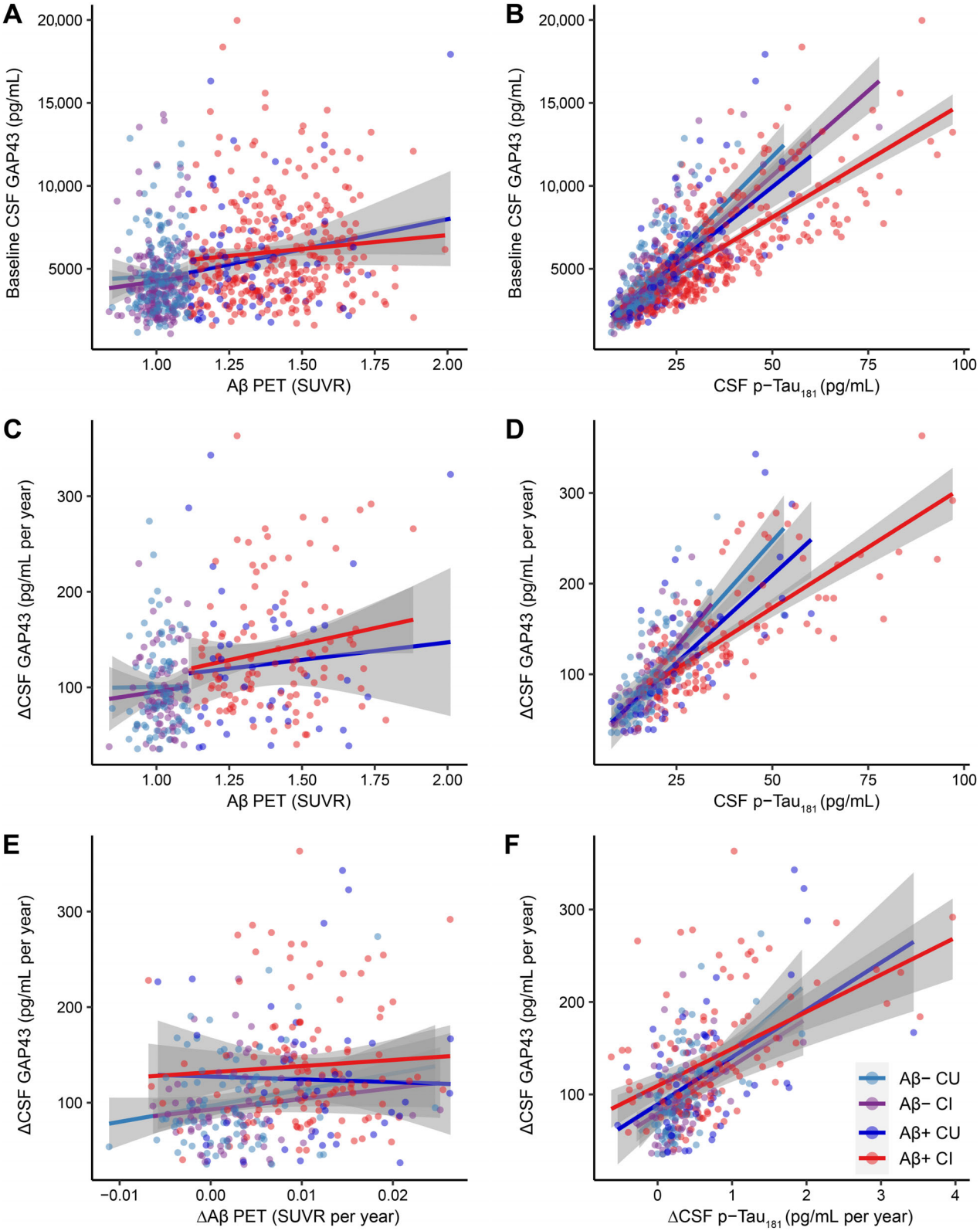


**FIGURE 3: Association of CSF GAP43 with Aβ PET and CSF p-Tau in different Aβ PET and cognitive status. Associations of baseline CSF GAP43 with (A) baseline Aβ PET and (B) baseline CSF p-Tau$_{181}$. Associations of CSF GAP43 slopes (ΔCSF GAP43) with (C) baseline Aβ PET, (D) baseline CSF p-Tau$_{181}$, (E) Aβ PET slopes (ΔAβ PET), and (F) CSF p-Tau$_{181}$ slopes (ΔCSF p-Tau$_{181}$). The points and solid lines represent each group's individuals and regression lines, adjusting for age, sex, and *APOE*-ε4 status. Aβ = β-amyloid; CSF = cerebrospinal fluid; GAP43 = growth-associated protein-43; PET = positron emission tomography; p-Tau = phosphorylated tau.**

ΔPACC scores ($\beta_{std}$ = −0.19 [95% CI −0.30 to −0.09], $p$ < 0.001). However, no significant association was found between ΔCSF p-Tau$_{181}$ and ΔFDG PET among 233 individuals with concurrent longitudinal CSF p-Tau$_{181}$ and FDG PET data ($\beta_{std}$ = −0.10 [95% CI −0.23 to 0.03], $p$ = 0.116). We further conducted a mediation analysis to

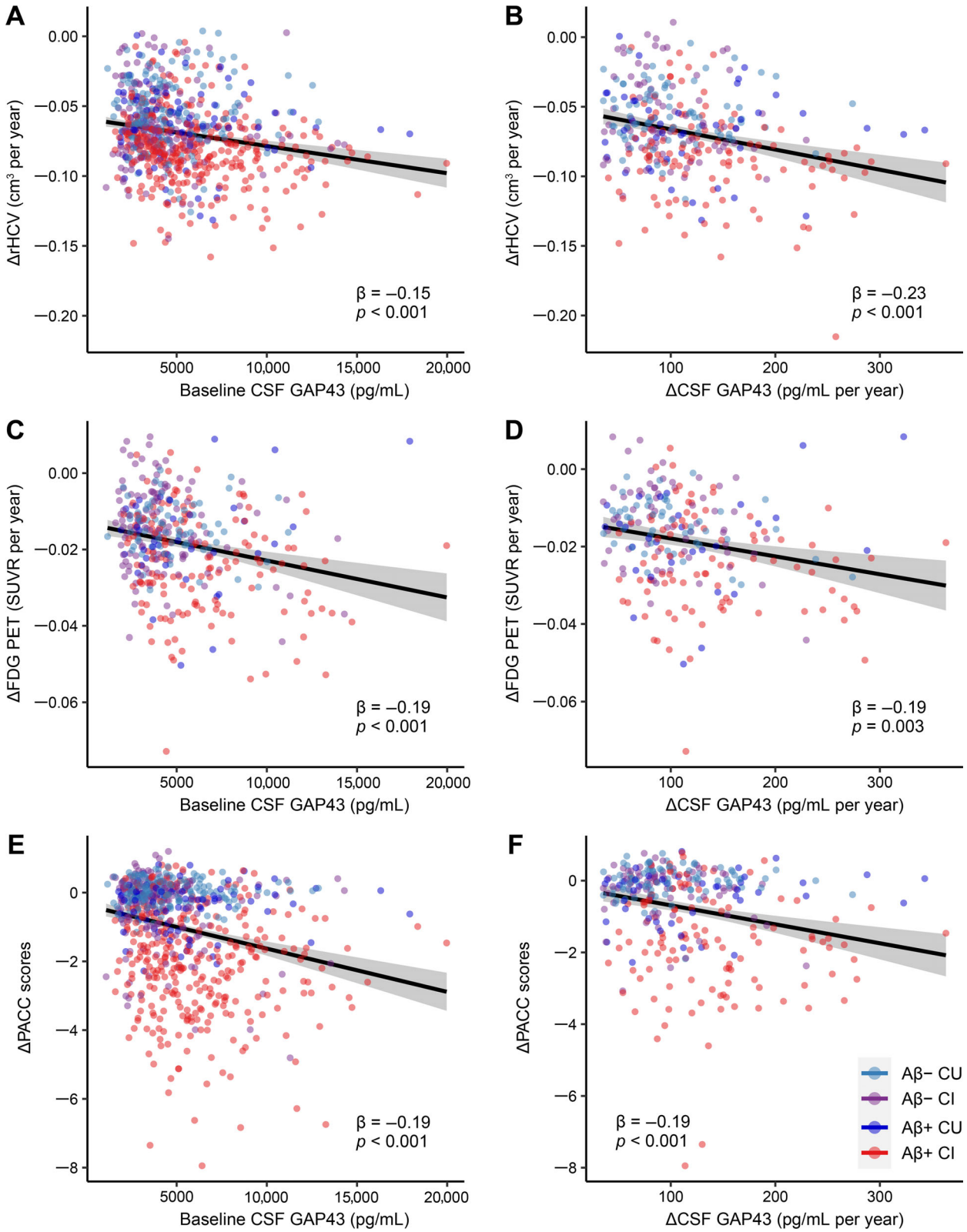


**FIGURE 4: Association of CSF GAP43 with longitudinal neurodegeneration and cognitive decline.** Associations of baseline CSF GAP43 with longitudinal changes of (A) rHCV (ΔrHCV), (C) FDG PET (ΔFDG PET), and (E) PACC scores (ΔPACC scores). Associations of CSF GAP43 slope (ΔCSF GAP43) with (B) ΔrHCV, (D) ΔFDG PET, and (F) ΔPACC scores. The points and solid lines represent the individuals and regression lines, respectively. The standardized regression coefficients (β) and *p* values were computed using a linear model across all individuals, adjusting for age, sex, and *APOE*-ε4 status. CSF = cerebrospinal fluid; FDG = $^{18}$F-fluorodeoxyglucose; GAP43 = growth-associated protein-43; PACC = preclinical Alzheimer cognitive composite; PET = positron emission tomography; rHCV = residual hippocampal volume

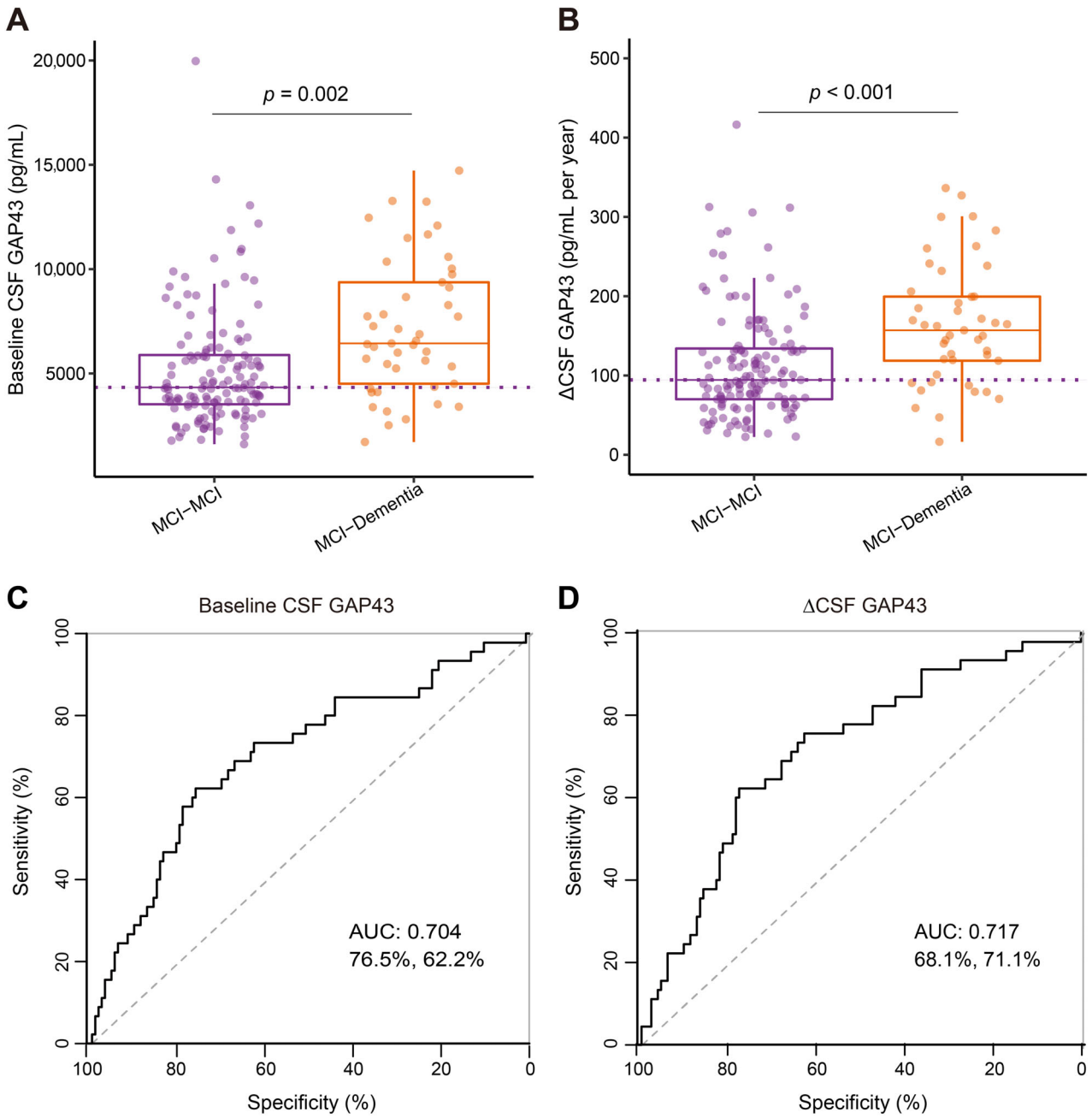


**FIGURE 5: Association between CSF GAP43 and clinical progression of MCI patients. Comparison of (A) baseline CSF GAP43 and (B) slopes of CSF GAP43 (ΔCSF GAP43) between MCI-MCI and MCI-dementia patients. Receiver operating characteristic curve analysis for differentiating individuals with progressing MCI from those with stable MCI using (C) baseline CSF GAP43 and (D) ΔCSF GAP43.The boxplots show the median (horizontal bar), interquartile range (IQR; hinges), and 1.5 × IQR (whiskers). The dots represent individual points of each group. The *p* values of the comparisons are shown at the top, adjusting for age, sex, and *APOE*-ε4 status. Dashed lines represent the median values of the MCI-MCI patients. AUC = area under the curve; CSF = cerebrospinal fluid; GAP43 = growth-associated protein-43; MCI = mild cognitive impairment.**

determine the sequential associations among ΔCSF p-Tau181 increases, ΔCSF GAP43 increases, ΔrHCV decreases, and ΔPACC decreases, and found that ΔCSF GAP43 and ΔrHCV significantly mediated the associations between ΔCSF p-Tau181 and ΔPACC scores (Fig 6A), suggesting that tau-related presynaptic dysfunction is driving neurodegeneration and cognitive decline (Fig 6B). To strengthen the mediation effect in AD etiology, we re-ran the results using the same mediation analysis when Aβ– CI participants were excluded from our model. The outcomes were largely the same.

## Discussion

In this study, we investigated the alterations of CSF GAP43 in different clinical and biological stages of AD,

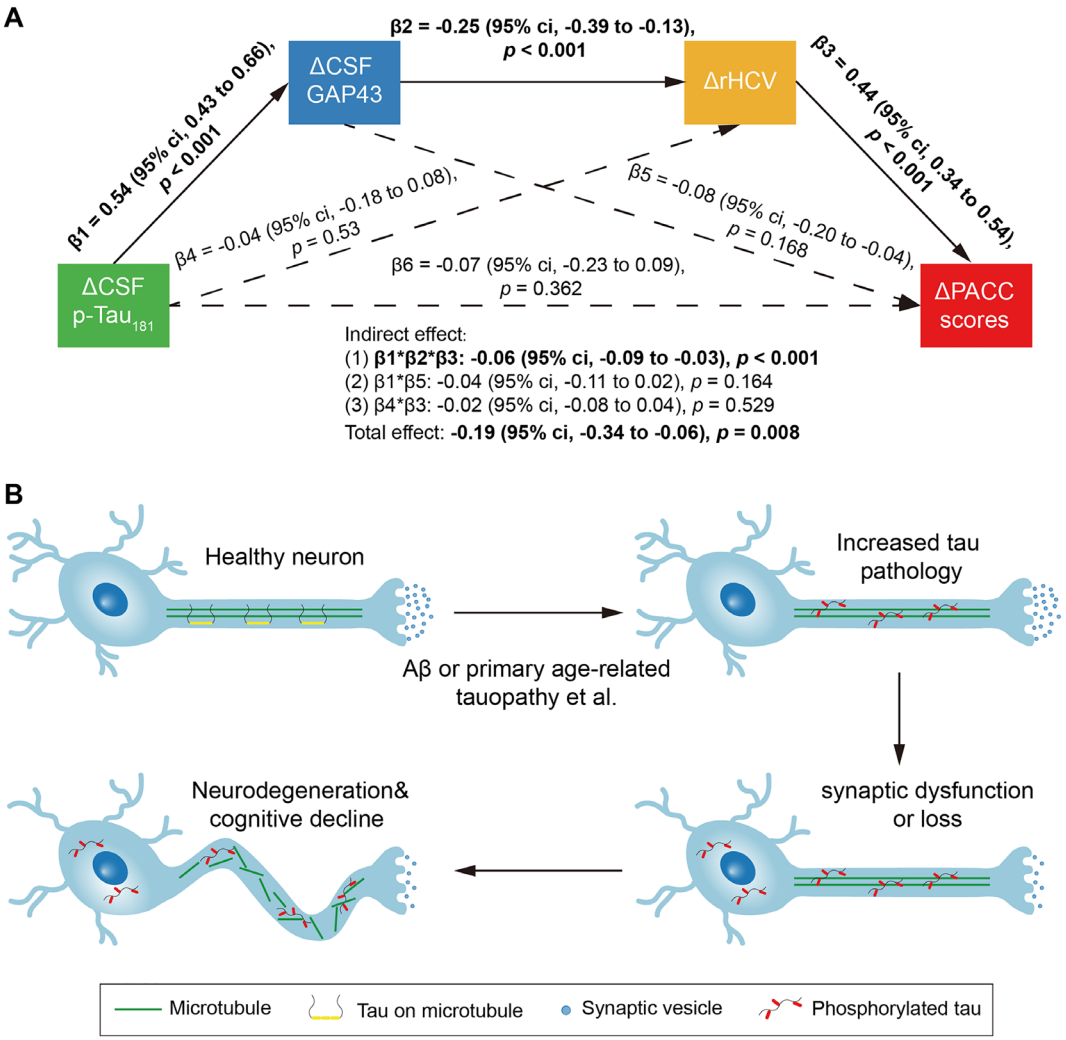


**FIGURE 6: Sequential association among longitudinal changes of CSF p-Tau$_{181}$, CSF GAP43, hippocampal atrophy, and cognitive decline. (A) CSF GAP43 slope (ΔCSF GAP43) and hippocampal atrophy slope (ΔrHCV) fully mediated the association between CSF p-Tau$_{181}$ slope (ΔCSF p-Tau$_{181}$) and preclinical Alzheimer cognitive composite (PACC) score slope (ΔPACC). The solid and the dashed lines, respectively, show the significant and non-significant pathways. A 5,000-bootstrapping procedure computed total, direct, and indirect associations. (B) Schematic of the sequential cascade of tau aggregation, synaptic dysfunction, neurodegeneration, and cognitive decline in neurodegenerative disease. CSF = cerebrospinal fluid; GAP43 = growth-associated protein-43; p-Tau$_{181}$ = phosphorylated tau181.**

and how they relate to Aβ, tau, neurodegeneration, and cognitive decline cross-sectionally and longitudinally. CSF p-Tau$_{181}$-positive individuals showed higher CSF GAP43 concentrations and faster rates of CSF GAP43 increases than CSF p-Tau$_{181}$-negative individuals regardless of Aβ positivity and cognitive status. Multivariate regression analyses extended these findings by showing that CSF GAP43 correlated positively with the CSF p-Tau$_{181}$ in both cross-sectional and longitudinal cohorts, independent of the Aβ PET profile. Furthermore, the longitudinal MRI and cognition data revealed that higher CSF GAP43 concentrations and faster rates of CSF GAP43 increases were associated with longitudinal decreases in hippocampal volume, glucose metabolism, and cognition. Finally, the mediation analyses demonstrated that more rapid rates of GAP43 increases significantly mediated the longitudinal associations among CSF p-Tau$_{181}$, hippocampal atrophy, and cognitive decline. Altogether, these findings suggest that elevated tau pathology rather than Aβ plaque is closely related to presynaptic dysfunction measured by CSF GAP43, which can lead to subsequent neurodegeneration and cognitive decline.

In line with the present findings, previous cross-sectional studies reported higher CSF GAP43 concentrations in patients with MCI[24, 34] or dementia[22] compared with the CU individuals. However, they did not stratify participants by Aβ status nor did they investigate longitudinal changes of CSF GAP43. We found higher CSF GAP43 concentrations in Aβ– dementia, Aβ+ MCI, and Aβ+ dementia groups than in the Aβ– CU group.

Longitudinally, we observed significantly faster CSF GAP43 increases in Aβ+ MCI individuals than in the Aβ– CU controls. We also observed marginally higher CSF GAP43 concentrations in Aβ+ CU individuals, in accordance with the results reported by two recent cross-sectional studies.[34, 35] Together, CSF GAP43 may likely increase in both symptomatic AD patients and people with suspected non-AD dementia.

Among different biological stages of AD, we found that CSF p-Tau$_{181}$-positive individuals (A−/T + or A + /T +) had both higher CSF GAP43 concentrations and faster rates of CSF GAP43 increases compared with the A−/T− or A + /T− individuals, regardless of clinical status. One recent study reported that tau-positive MCI patients had higher CSF GAP43 concentrations than the tau-negative MCI patients, which was in accordance with the present results.[24] However, another recently important study found elevated CSF GAP43 concentrations in A + /T− individuals than in the A−/T− individuals.[25] Notably, they defined abnormal tau positivity using tau PET imaging, which may be a relatively later biomarker of the formation of tau aggregation than CSF p-Tau according to previous reports by our group[5] and other laboratories.[36, 37] Importantly, the multivariate regression analyses in the present study provide further evidence for explaining that CSF GAP43 increases were positively associated with tau pathology rather than Aβ plaques in both cross-sectional and longitudinal analyses, regardless of Aβ positivity and cognitive status. In contrast, two cross-sectional studies found CSF GAP43 was associated with Aβ and tau pathologies, but they did not analyze their independent effect.[22, 23] Recently, another two cross-sectional studies reported no association between Aβ pathology and CSF GAP43 when controlling for CSF p-Tau,[24, 35] supporting the findings in the present study. Together with our results and previous literature, the presynaptic dysfunction measured by CSF GAP43 may be closely linked to tau pathology independent of cortical Aβ deposition and clinical diagnosis.

The substantial synaptic loss may contribute to neurodegeneration in the brain, leading to cognitive impairment.[15, 38, 39] Thus, we subsequently explored the predictive effects of CSF GAP43 on longitudinal hippocampal atrophy, hypometabolism, and cognitive decline. This showed that CSF GAP43 was associated with more rapid hippocampal atrophy and cognitive decline, especially in symptomatic AD, as well as hypometabolism. Additionally, in a subgroup of MCI patients with follow-up clinical assessments, we found that higher CSF GAP43 concentrations and faster rates of CSF GAP43 increases could identify progressing MCI individuals with >70% AUC values. Consistent with the present findings, higher CSF GAP43 concentrations were reported to be negatively associated with cortical thickness[35] and cognition.[22] However, in contrast to the present study, one cross-sectional study found elevated CSF GAP43 concentrations were weakly related to higher glucose metabolism, which may be explained by the fact that they focused on preclinical AD individuals.[35] Notably, previous studies[40, 41] showed that brain metabolism hyperactivity appeared to be detected in some brain regions in the early stage of AD, which could be driven by activated microglial.[42] Previous studies reported that CSF p-Tau was significantly related to neurodegeneration and cognitive decline.[43–45] Intriguingly, our mediation analysis provided further novel findings that presynaptic dysfunction measured by CSF GAP43 fully mediated the associations of CSF p-Tau$_{181}$ increases with longitudinal hippocampal atrophy and cognitive decline.

Given the close relationship between synaptic function and cognition, the very early response of presynapse to pathological tau changes emphasizes the importance of therapeutic strategies targeting tau pathology at the presymptomatic stage in clinical trials, which may contribute to diminishing synaptic impairment and ameliorating cognition. Furthermore, the present results suggest that CSF GAP43 could be used as an indirect biomarker of presynapse for evaluating the progression of synaptic pathology in patients and monitoring the exacerbation of neurodegenerative dementia in clinical practice. Despite the annual changes of CSF GAP43 being gentle and consistent with previous longitudinal studies of other CSF biomarkers, we found that more rapid increases in CSF GAP43 were related to faster hippocampal atrophy, hypometabolism, and cognitive decline.[46, 47] Nonetheless, additional longitudinal studies based on different cohorts are critical to confirm the longitudinal changes in CSF GAP43.

In the present study, we used a large dataset to explore the abnormal changes of presynaptic protein measured by CSF GAP43 among different stages of AD, and how presynaptic loss relates to Aβ plaques, CSF p-Tau$_{181}$, hippocampal atrophy, hypometabolism, and cognitive decline. These findings might provide novel insights into understanding the role of presynaptic loss in AD, and extend current A/T/N biomarkers to detect neurodegenerative diseases.

However, this study had some limitations, as follows. We selected CSF p-Tau$_{181}$ to represent tau pathology, which may be inferior to other phosphorylation sites (such as p-Tau$_{217}$,[48, 49] which is not available in ADNI), and these findings still require further investigation in tau PET imaging.[50] Although CSF GAP43 was related to tau pathology measured by CSF p-Tau$_{181}$, the current study is correlational in nature and does not test CSF p-Tau$_{181}$

or CSF GAP43 changes as a causal event. All we can confirm is that there seems to be an association with processes that result in elevated CSF p-Tau$_{181}$ and GAP43. Autopsy confirmation would be required in the future. In addition, this cohort lacks other synapse-related biomarkers (such as presynaptic protein SNAP-25 and postsynaptic protein neurogranin, whose sample sizes in the ADNI cohort are limited), which may reflect the different mechanism of synapse degeneration occurring in various stages of the disease. Additional confirmation is still required by using other synaptic proteins. Finally, the longitudinal data of CSF GAP43 and FDG PET were limited, which may need to be validated by further longitudinal data with more visits and longer follow-up periods.

In conclusion, the present study provides novel insights into the association of presynaptic loss with Aβ, tau, neurodegeneration, and cognitive decline, where elevated tau pathology is driving presynaptic dysfunction or loss, resulting in subsequent neurodegeneration and cognitive decline. The tau-related presynaptic protein, GAP43, in CSF may be a promising biomarker for synaptic damage. It can strengthen the measurement of neurodegeneration beyond the current commonly-used neurodegeneration biomarkers, which may provide more information to understand the characteristics and progression of neurodegenerative diseases.

## Acknowledgments

This work was supported by the National Natural Science Foundation of China (82171197), the Shenzhen Bay Laboratory Key Project (S211101002-2), and the Shenzhen Bay Laboratory Open Project (SZBL2020090501014).

The authors thank all the ADNI participants and staff for their contributions to data acquisition. The Data collection and sharing for this project were funded by the ADNI (National Institutes of Health Grant U01 AG024904) and DOD ADNI (Department of Defense award number W81XWH-12-2-0012). ADNI is funded by the National Institute on Aging, the National Institute of Biomedical Imaging and Bioengineering, and through generous contributions from the following: AbbVie, Alzheimer's Association; Alzheimer's Drug Discovery Foundation; Araclon Biotech; BioClinica, Inc.; Biogen; Bristol-Myers Squibb Company; CereSpir, Inc.; Eisai Inc.; Elan Pharmaceuticals, Inc.; Eli Lilly and Company; EuroImmun; F. Hoffmann-La Roche Ltd and its affiliated company Genentech, Inc.; Fujirebio; GE Healthcare; IXICO Ltd.; Janssen Alzheimer Immunotherapy Research & Development, LLC.; Johnson & Johnson Pharmaceutical Research & Development LLC.; Lumosity; Lundbeck; Merck & Co., Inc.; Meso Scale Diagnostics, LLC.; NeuroRx Research; Neurotrack Technologies; Novartis Pharmaceuticals Corporation; Pfizer Inc.; Piramal Imaging; Servier; Takeda Pharmaceutical Company; and Transition Therapeutics. The Canadian Institutes of Health Research is providing funds to support ADNI clinical sites in Canada. Private sector contributions are facilitated by the Foundation for the National Institutes of Health (www.fnih.org). The grantee organization is the Northern California Institute for Research and Education, and the study is coordinated by the Alzheimer's Disease Cooperative Study at the University of California, San Diego. ADNI data are disseminated by the Laboratory for Neuro Imaging at the University of Southern California.

## Author Contributions

T.G. and G.L. contributed to the conception and design of the study; T.G., G.L., Y.C., and A.L. contributed to the acquisition and analysis of data; T.G., G.L., Z.L., and S.M. contributed to drafting the manuscript and preparing the figures.

## Potential Conflicts of Interest

Nothing to report.

### *Data Availability*

All data used in the current study were obtained from the ADNI database (available at https://adni.loni.usc.edu). Derived data are available from the corresponding author on request by any qualified investigator subject to a data use agreement.

## References

1. Jagust W. Imaging the evolution and pathophysiology of Alzheimer disease. Nat Rev Neurosci 2018;19:687–700.
2. Guo T, Brendel M, Grimmer T, et al. Predicting regional pattern of longitudinal β-amyloid accumulation by baseline PET. J Nucl Med 2017;58:639–645.
3. Schöll M, Lockhart SN, Schonhaut DR, et al. PET imaging of tau deposition in the aging human brain. Neuron 2016;89:971–982.
4. Guo T, Shaw LM, Trojanowski JQ, et al. Association of CSF Aβ, amyloid PET, and cognition in cognitively unimpaired elderly adults. Neurology 2020;95:e2075–e2085.
5. Guo T, Korman D, La Joie R, et al. Normalization of CSF pTau measurement by Aβ40improves its performance as a biomarker of Alzheimer's disease. Alzheimer's Res Ther 2020;12:97.
6. Jack CR, Bennett DA, Blennow K, et al. NIA-AA research framework: toward a biological definition of Alzheimer's disease. Alzheimers Dement 2018;14:535–562.
7. Jack CR, Wiste HJ, Therneau TM, et al. Associations of amyloid, tau, and neurodegeneration biomarker profiles with rates of memory decline among individuals without dementia. JAMA 2019;321:2316–2325.

8. Guo T, Korman D, Baker SL, et al. Longitudinal cognitive and biomarker measurements support a unidirectional pathway in Alzheimer's disease pathophysiology. Biol Psychiatry 2021;89: 786–794.
9. Dodich A, Mendes A, Assal F, et al. The A/T/N model applied through imaging biomarkers in a memory clinic. Eur J Nucl Med Mol Imaging 2020;47:247–255.
10. Ebenau JL, Timmers T, Wesselman LMP, et al. ATN classification and clinical progression in subjective cognitive decline. Neurology 2020; 95:e46–e58.
11. Altomare D, de Wilde A, Ossenkoppele R, et al. Applying the ATN scheme in a memory clinic population: the ABIDE project. Neurology 2019;93:e1635–e1646.
12. Burke BT, Latimer C, Keene CD, et al. Theoretical impact of the AT(N) framework on dementia using a community autopsy sample. Alzheimers Dement 2021;17:1879–1891.
13. Ingala S, De Boer C, Masselink LA, et al. Application of the ATN classification scheme in a population without dementia: findings from the EPAD cohort. Alzheimers Dement 2021;17:1189–1204.
14. Hampel H, Cummings J, Blennow K, et al. Developing the ATX(N) classification for use across the Alzheimer disease continuum. Nat Rev Neurol 2021;17:580–589.
15. Chen Y, Fu AKY, Ip NY. Synaptic dysfunction in Alzheimer's disease: mechanisms and therapeutic strategies. Pharmacol Ther 2019;195: 186–198.
16. De Wilde MC, Overk CR, Sijben JW, Masliah E. Meta-analysis of synaptic pathology in Alzheimer's disease reveals selective molecular vesicular machinery vulnerability. Alzheimers Dement 2016;12: 633–644.
17. Forner S, Baglietto-Vargas D, Martini AC, et al. Synaptic impairment in Alzheimer's disease: a dysregulated symphony. Trends Neurosci 2017;40:347–357.
18. Neve RL, Finch EA, Bird ED, Benowitz LI. Growth-associated protein GAP-43 is expressed selectively in associative regions of the adult human brain. Proc Natl Acad Sci 1988;85:3638–3642.
19. Benowitz L, Perrone-Bizzozero N, Finklestein S, Bird E. Localization of the growth-associated phosphoprotein GAP-43 (B-50, F1) in the human cerebral cortex. J Neurosci 1989;9:990–995.
20. Davidsson P, Blennow K. Neurochemical dissection of synaptic pathology in Alzheimer's disease. Int Psychogeriatr 1998;10:11–23.
21. Bogdanovic N, Davidsson P, Volkmann I, et al. Growth-associated protein GAP-43 in the frontal cortex and in the hippocampus in Alzheimer's disease: an immunohistochemical and quantitative study. 2000.
22. Sandelius Å, Portelius E, Källén Å, et al. Elevated CSF GAP-43 is Alzheimer's disease specific and associated with tau and amyloid pathology. Alzheimers Dement 2019;15:55–64.
23. Tible M, Sandelius Å, Höglund K, et al. Dissection of synaptic pathways through the CSF biomarkers for predicting Alzheimer disease. Neurology 2020;95:e953–e961.
24. Bergström S, Remnestål J, Yousef J, et al. Multi-cohort profiling reveals elevated CSF levels of brain-enriched proteins in Alzheimer's disease. Ann Clin Transl Neurol 2021;8:1456–1470.
25. Pereira JB, Janelidze S, Ossenkoppele R, et al. Untangling the association of amyloid-β and tau with synaptic and axonal loss in Alzheimer's disease. Brain 2021;144:310–324.
26. Hansson O, Seibyl J, Stomrud E, et al. CSF biomarkers of Alzheimer's disease concord with amyloid-β PET and predict clinical progression: a study of fully automated immunoassays in BioFINDER and ADNI cohorts. Alzheimers Dement 2018;14:1470–1481.
27. Desikan RS, Ségonne F, Fischl B, et al. An automated labeling system for subdividing the human cerebral cortex on MRI scans into gyral based regions of interest. Neuroimage 2006;31:968–980.
28. Landau SM, Fero A, Baker SL, et al. Measurement of longitudinal β-amyloid change with 18 F-Florbetapir PET and standardized uptake value ratios. J Nucl Med 2015;56:567–574.
29. Landau SM, Mintun MA, Joshi AD, et al. Amyloid deposition, hypometabolism, and longitudinal cognitive decline. Ann Neurol 2012;72:578–586.
30. Jack CR, Knopman DS, Weigand SD, et al. An operational approach to National Institute on Aging-Alzheimer's Association criteria for preclinical Alzheimer disease. Ann Neurol 2012;71:765–775.
31. Schindler SE, Gray JD, Gordon BA, et al. Cerebrospinal fluid biomarkers measured by Elecsys assays compared to amyloid imaging. Alzheimers Dement 2018;14:1460–1469.
32. Donohue MC, Sperling RA, Salmon DP, et al. The preclinical Alzheimer cognitive composite: measuring amyloid-related decline. JAMA Neurol 2014;71:961–970.
33. Rosseel Y. Lavaan: an R package for structural equation modeling. J Stat Softw 2012;48:1–93.
34. Remnestål J, Just D, Mitsios N, et al. CSF profiling of the human brain enriched proteome reveals associations of neuromodulin and neurogranin to Alzheimer's disease. Proteomics 2016;10:1242–1253.
35. Milà-Alomà M, Brinkmalm A, Ashton NJ, et al. CSF synaptic biomarkers in the preclinical stage of Alzheimer disease and their association with MRI and PET: a cross-sectional study. Neurology 2021; 97:e2065–e2078. https://doi.org/10.1212/WNL.0000000000012853.
36. Meyer P-F, Pichet Binette A, Gonneaud J, et al. Characterization of Alzheimer disease biomarker discrepancies using cerebrospinal fluid phosphorylated tau and AV1451 positron emission tomography. JAMA Neurol 2020;77:508–516.
37. Mattsson-Carlgren N, Andersson E, Janelidze S, et al. Aβ deposition is associated with increases in soluble and phosphorylated tau that precede a positive tau PET in Alzheimer's disease. Sci Adv 2020;6: eaaz2387.
38. Terry RD, Masliah E, Salmon DP, et al. Physical basis of cognitive alterations in Alzheimer's disease: synapse loss is the major correlate of cognitive impairment 1991.
39. Jacobs J, Kahana MJ. Direct brain recordings fuel advances in cognitive electrophysiology. Trends Cogn Sci 2010;14:162–171.
40. Johnson SC, Christian BT, Okonkwo OC, et al. Amyloid burden and neural function in people at risk for Alzheimer's disease. Neurobiol Aging 2014;35:576–584.
41. Oh H, Habeck C, Madison C, Jagust W. Covarying alterations in Aβ deposition, glucose metabolism, and gray matter volume in cognitively normal elderly. Hum Brain Mapp 2014;35:297–308.
42. Xiang X, Wind K, Wiedemann T, et al. Microglial activation states drive glucose uptake and FDG-PET alterations in neurodegenerative diseases. Sci Transl Med 2021;13:eabe5640.
43. Barthélemy NR, Li Y, Joseph-Mathurin N, et al. A soluble phosphorylated tau signature links tau, amyloid and the evolution of stages of dominantly inherited Alzheimer's disease. Nat Med 2020;26: 398–407.
44. Llibre-Guerra JJ, Li Y, Schindler SE, et al. Association of Longitudinal Changes in cerebrospinal fluid Total tau and phosphorylated tau 181 and brain atrophy with disease progression in patients with Alzheimer disease. JAMA Netw Open 2019;2: e1917126.
45. Pascoal TA, Mathotaarachchi S, Shin M, et al. Synergistic interaction between amyloid and tau predicts the progression to dementia. Alzheimers Dement 2017;13:644–653.
46. Kester MI, Teunissen CE, Crimmins DL, et al. Neurogranin as a cerebrospinal fluid biomarker for synaptic loss in symptomatic Alzheimer disease. JAMA Neurol 2015;72:1275–1280.
47. Lleó A, Alcolea D, Martínez-Lage P, et al. Longitudinal cerebrospinal fluid biomarker trajectories along the Alzheimer's disease continuum in the BIOMARKAPD study. Alzheimers Dement 2019;15:742–753.

48. Janelidze S, Stomrud E, Smith R, et al. Cerebrospinal fluid p-tau217 performs better than p-tau181 as a biomarker of Alzheimer's disease. Nat Commun 2020;11:1683.

49. Leuzy A, Janelidze S, Mattsson-Carlgren N, et al. Comparing the clinical utility and diagnostic performance of cerebrospinal fluid P-Tau181, P-Tau217 and P-Tau231 assays. Neurology 2021;97:e1681–e1694. https://doi.org/10.1212/WNL.0000000000012727.

50. Ossenkoppele R, Reimand J, Smith R, et al. Tau PET correlates with different Alzheimer's disease-related features compared to CSF and plasma p-tau biomarkers. EMBO Mol Med 2021;13:1–15.